RAA 2014 Vol. **14** No. **7**, 864–868 doi: 10.1088/1674–4527/14/7/008
http://www.raa-journal.org *http://www.iop.org/journals/raa*

Research in Astronomy and Astrophysics

A 96-antenna radioheliograph

Sergey V. Lesovoi, Alexander T. Altyntsev, Eugene F. Ivanov and Alexey V. Gubin

Institute of Solar-Terrestrial Physics, Irkutsk 664033, Russia; *svlesovoi@gmail.com*

Received 2014 January 2; accepted 2014 March 18

Abstract Here we briefly present some design approaches for a multifrequency 96-antenna radioheliograph. The configuration of the array antenna, transmission lines and digital receivers is the main focus of this work. The radioheliograph is a T-shaped centrally condensed radiointerferometer operating in the frequency range 4–8 GHz. The justification for the choice of such a configuration is discussed. The signals from antennas are transmitted to a workroom by analog optical links. The dynamic range and phase errors of the microwave-over-optical signal are considered. The signals after downconverting are processed by digital receivers for delay tracking and fringe stopping. The required step of delay tracking and data rates are considered. Two 3-bit data streams (I and Q) are transmitted to a correlator with the transceivers embedded in Field Programmed Gate Array chips and with PCI Express cables.

Key words: telescopes — instrumentation: interferometers — Sun: radio radiation

1 INTRODUCTION

The development of the next-generation, ground-based solar radio telescopes is aimed at finding a solution to current problems in solar-terrestrial physics. A few next generation radioheliographs are under construction. The main objective of such instruments is imaging the Sun with both good spatial and spectral resolutions. The Chinese Spectral Radioheliograph (CSRH) is being constructed in the Inner Mongolia region of China (Yan et al. 2011, 2013). CSRH I (0.4–2.0 GHz) is now undergoing tests, and the infrastructure for CSRH II (2–15 GHz) is being laid. The Expanded Owens Valley Solar Array has been operating in the frequency range 1–9 GHz in order to test design elements (Gary et al. 2012) and is now nearing completion with operation in the range 2.5–18 GHz. The 96-antenna multifrequency radioheliograph is currently under construction. This radioheliograph is an upgrade of the Siberian Solar Radio Telescope (SSRT) (Grechnev et al. 2003). Advantages of the radioheliograph design were discussed in the description of the 10-antenna prototype (Lesovoi et al. 2012). Here we focus on some of the key features that need to be emphasized. In this work we would like to consider the following issues: the antenna configuration, the dynamic range and phase errors of the analog optical links and the required step of delay tracking.

2 ANTENNA CONFIGURATION

Because the existing antenna stations of the SSRT are used for the radioheliograph antennas, the antenna configuration of the radioheliograph is a T-shaped centrally condensed array. The shortest baseline is 4.9 m, while the longest are 622.30 m and 311.15 m in the East-West and South directions respectively. The varying distance between adjacent antennas is determined not only by considering

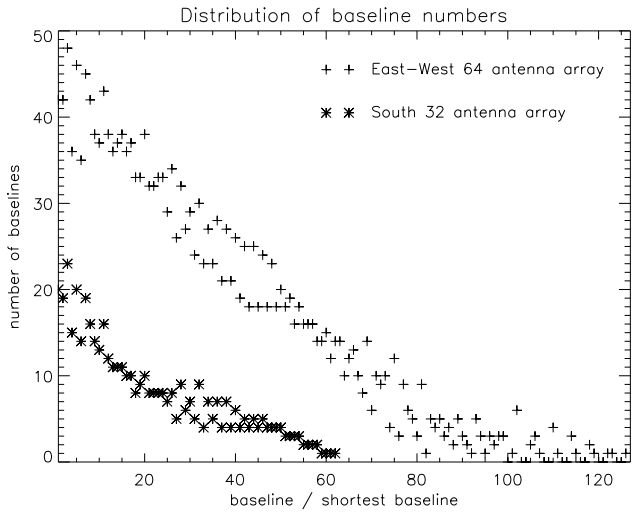

Fig. 1 Distribution of one-dimensional baselines for the South and East-West antenna arrays of the radioheliograph. With the exception of four baselines in the South array and 11 in the East-West array, all baselines are redundant.

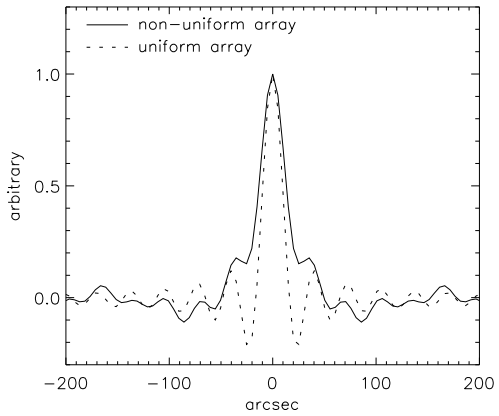

Fig. 2 Point spread functions of both non-uniform and uniform arrays. Sidelobe levels are comparable in the vicinity of the main lobe.

the point spread function (PSF) but also the requirement to fit 32 antennas in each arm of the T-shaped array. The total number of baselines in the 96-antenna radioheliograph is 4560.

Figure 1 shows the distribution of 2512 one-dimensional baselines along the East-West and South directions. These baselines are redundant except for four baselines in the South array and 11 baselines in the East-West array. The responses of these baselines to the solar microwave signal will be used to calibrate the antenna phases and magnitudes. The total number of non-redundant two-dimensional baselines used to image the Sun is 2048.

The East-West cross section of the two-dimensional PSF of the radioheliograph is shown in Figures 2 and 3. It is distinctly seen from Figures 2 and 3 that the levels of sidelobes for the non-

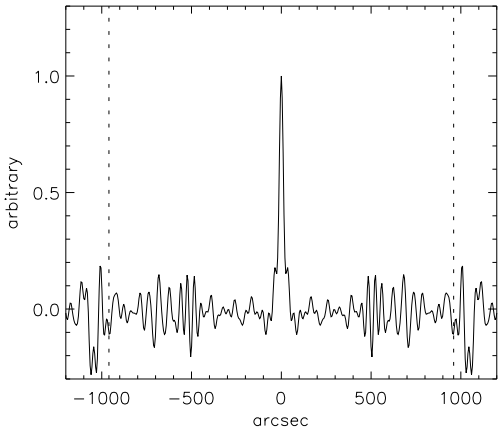

Fig. 3 Point spread function of the non-uniform array. Dashed lines show the angular size of the Sun. The sidelobe level significantly increases with distance from the main lobe.

uniform (centrally condensed) and uniform arrays are only comparable in the vicinity of the main lobe. The high level of far sidelobes is one reason to use a uniform array, because more precision is required to calculate far sidelobes in the dirty PSF. Although the uniform array has better spatial resolution and, especially, distant sidelobe performance than the centrally condensed array, nevertheless the added expense is prohibitive.

3 ANALOG FIBER OPTICAL LINKS

An analog optical link with direct modulation of a laser diode is used for transmission of the radio frequency (RF) signal from an antenna to the workroom. Compensation of the high losses in the analog optical link is provided by using an RF preamplifier. However, the dynamic range and the phase errors in the RF signal should be considered. The typical spur free dynamic range (SFDR) (3rd order) of the analog optical link is about SFDR_3=100 dB $\mathrm{Hz}^{2/3}$. The dynamic range for a bandwidth of 4 GHz will be $\mathrm{SFDR}_{3\Delta f} = \mathrm{SFDR}_3 - 2/3 \times 10 \times \lg(4 \times 10^9) \approx 36$ dB. The fluxes of the quiet Sun are about 200 s.f.u. for the operating frequency range of 4–8 GHz. So, it is possible to observe microwave bursts with a peak flux of up to $4{\times}10^5$ s.f.u. Because the occurrence of such high peak flux bursts is negligible (Nita et al. 2002), it is not necessary to use a switched attenuator at the antenna front end for observations of solar flares.

The sources of the phase errors in the RF signal, after its conversion from optical to electrical form, are the finite spectral width of the laser emission and chromatic dispersion of the fiber. The spectral width of the semiconductor single mode laser is about 0.5 nm. The typical chromatic dispersion of the fiber near the wavelength 1310 nm is about 1 ps/(km nm). The length of the optical link in our design is about 0.4 km, which leads to a delay error of 0.2 ps. The phase error at the frequency of 6 GHz will be about 0.5°, which is acceptable. The temperature dependence of the transmission delay also leads to a phase error in microwaves. The typical temperature drift of the delay is about 40–130 ps/(km °C). The local change in diurnal temperature is about 20°C and the fact that only about 5 m of optical cable lay outdoors results in a diurnal change in delay of about 10 ps. The phase change at the frequency of 6 GHz is about 20° per day. The correlation is affected only by the difference of antenna phases. One can expect these differences will be much less relative to phase errors, i.e. about 2° per day, which is acceptable.

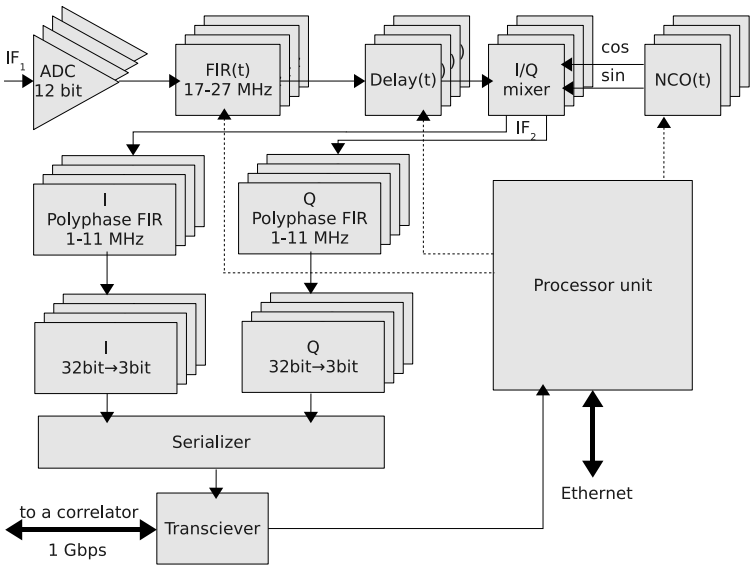

Fig. 4 Digital receiver module for four antennas. Two 3-bit streams (I, Q) are transmitted to a correlator with the transceiver in the basic functional mode.

4 DIGITAL RECEIVERS

Each digital receiver module (Fig. 4) in the radioheliograph processes signals from four antennas. It converts signals at the first intermediate frequency to digital data and forms a passband at 17–27 MHz. The 64-th order finite impulse response filter (FIR) is used both to form the passband and for fractional-sample delay. The digital downconvertor is used simultaneously to produce IQ signals, for fringe stopping and to downconvert IF_1 signals to a second intermediate frequency passband 1–11 MHz (IF_2). The data rate required for transmission from the digital receiver to a correlator can be two times less due to such an IF_2 passband. So, the instantaneous frequency bandwidth (i.e. spectral resolution) of the radioheliograph is 10 MHz. The number of frequency channels is only limited by the desired temporal resolution. Because the integration time is about 0.1 s, the temporal resolution for the case of 100 frequency channels is about 10 s. The delay errors result in an error in the phase slope of the signal, denoted as IF_2, and defined by

$$2\pi\nu_{if2}\left(\delta\tau_g^k - \delta\tau_g^l\right) = 2\pi\nu_{if2}\Delta\tau_g^{kl}\,,$$

where

$$\delta\tau_g^k = \tau_g^k - n\tau_{\rm step}$$

and

$$\delta\tau_g^l = \tau_g^l - m\tau_{\rm step}$$

are delays errors for antennas k and l, and $\tau_{\rm step}$ is a discrete step in the instrumental delay. The rms frequency within the passband is $\Delta\nu_{if2}/2\sqrt{3}$. Because the rms delay error is $\tau_{\rm step}/6$ (Thompson et al. 2001), one can infer that the phase error is $2\pi\frac{\Delta\nu_{if2}}{2\sqrt{3}}\frac{\tau_{\rm step}}{6} \leq 1^\circ$ for a delay step of 1 ns. However, the delay errors lead to significant displacements in the beam pattern of a two-element

interferometer respect to a single dish one

$$\Delta\theta = c\Delta\tau_g^{kl} / \left(|\boldsymbol{b^k} - \boldsymbol{b^l}| \sin\theta \right),$$

where $\boldsymbol{b^k}$ and $\boldsymbol{b^l}$ are baselines of antennas k and l, c is the speed of light and θ is the source angle. The angular displacement for a delay step of 1 ns for the shortest baseline at culmination is $\Delta\theta \approx 3.5^\circ$. This is excessive, and therefore the step for the fractional-sample delay is chosen as 0.1 ns. In practice, such a small delay step is sufficient to smooth phase jumps in correlations for the shortest baselines. The data from the 3-bit I and 3-bit Q digital receiver are transmitted to the correlator. The sampling rate of the data is 25 MHz. The net data rate for the whole receiver is 600 Msps and the data rate with payload bits is 800 Msps. Finally, the input data rate of the correlator after 8b/10b encoding should be 24 Gbps for 96 antennas. This data stream can be transmitted from the receiver modules to the correlator via transceivers embedded in Altera^{TM}Field Programmed Gate Array (FPGA) chips. A PCI Express over cable solution is used. More specifically, PCI Express cables and the transceivers in the basic functional mode are used. This solution allows calculation of all complex correlations for the 96-antenna interferometer with a single FPGA chip.

5 CONCLUSIONS

The antenna configuration, analog optical links and digital receivers of a 96-antenna radioheliograph are considered. The T-shaped antenna configuration is chosen because the existing antenna stations of the SSRT are used for the radioheliograph. The centrally condensed array is chosen because it is less expensive than an equivalent uniform array. It is shown that the SFDR of the analog optical links is sufficient to observe solar flares without using a switched attenuator. The phase errors and temperature drifts of the link are acceptable. Because of the short baselines (a few meters), typical for solar radiointerferometers, a delay tracking step of 0.1 ns is needed. Experience in implementation has shown that such a step can be realized with fractional sample delaying.

Acknowledgements We thank an anonymous referee for constructive comments. This study was supported by the Russian Foundation of Basic Research (12-02-91161, 12-02-00173, 12-02-10006 and 13-02-90472) and by a Marie Curie International Research Staff Exchange Scheme Fellowship within the 7th European Community Framework Programme. The work was supported in part by grants from the Ministry of Education and Science of the Russian Federation (State Contracts 16.518.11.7065 and 02.740.11.0576).

References

Gary, D. E., Nita, G. M., & Sane, N. 2012, Expanded Owens Valley Solar Array (EOVSA) Testbed and Prototype, in American Astronomical Society Meeting Abstracts #220, #204.30

Grechnev, V. V., Lesovoi, S. V., Smolkov, G. Y., et al. 2003, Sol. Phys., 216, 239

Lesovoi, S. V., Altyntsev, A. T., Ivanov, E. F., & Gubin, A. V. 2012, Sol. Phys., 280, 651

Nita, G. M., Gary, D. E., Lanzerotti, L. J., & Thomson, D. J. 2002, ApJ, 570, 423

Thompson, A. R., Moran, J. M., & Swenson, G. W., Jr. 2001, Interferometry and Synthesis in Radio Astronomy, 2nd Edition eds. A. Richard Thompson, James M. Moran, and George W. Swenson, Jr. (New York: Wiley)

Yan, Y., Wang, W., Liu, F., et al. 2013, Radio Imaging-spectroscopy Observations of the Sun in Decimetric and Centimetric Wavelengths, in IAU Symposium, 294, eds. A. G. Kosovichev, E. de Gouveia Dal Pino, & Y. Yan, 489

Yan, Y. H., Zhang, J., Chen, Z. J., et al. 2011, in General Assembly and Scientific Symposium, 2011 XXXth URSI, 1–4 (IEEE)